Prediction and Observation of Robust One-Way Bulk States in a Gyromagnetic Photonic Crystal

Jianfeng Chen[1] and Zhi-Yuan Li[1,2,*]

[1]School of Physics and Optoelectronics, South China University of Technology, Guangzhou 510640, China
[2]State Key Laboratory of Luminescent Materials and Devices, South China University of Technology, Guangzhou 510640, China

(Received 1 March 2022; accepted 26 May 2022; published 21 June 2022)

We report a two-dimensional heterogeneous Haldane model composed of alternately stacking modified Haldane lattices with opposite next-nearest-neighbor hoppings, and predict the emergence of robust one-way bulk states by an *ab initio* theoretical calculation. These unique bulk states transport unidirectionally and are robust against backscattering from impurities in the strip bulk. By analogy with the heterogeneous Haldane model, we further confirm by numerical simulations and experimental measurements the existence of robust one-way bulk states in a two-dimensional microwave gyromagnetic photonic crystal, and demonstrate their robust one-way property over a long-distance even in the presence of metallic obstacles. Our study provides the strong support for the generalization and application of band theories to fermionic and bosonic systems, and paves a way for the implementation of high-throughput robust energy transmission materials and devices.

DOI: 10.1103/PhysRevLett.128.257401

Introduction.—Among the unique and counterintuitive attributes of topological systems, topologically protected robust one-way transport is undoubtedly the most remarkable [1–3]. Topologically protected robust one-way transport was firstly found in electronic systems [1–4], which can be described by the celebrated Haldane model with time-reversal symmetry breaking. Later on, it was extended to various time-reversal symmetry invariant scenarios (e.g., Z_2 [5] and other symmetry-protected models [6–9]) and stimulated study of numerous classical analogs [10–14]. Topological phases of the celebrated Haldane model are generally characterized by chiral one-way edge states that are propagating in opposite directions at two parallel edges of a rectangular strip. These chiral edge states have been observed in classical quantum Hall effect electronic systems [1–4] and nonreciprocal manmade structures, such as externally dc-magnetically biased gyromagnetic photonic crystals [15,16] or acoustic [17] and mechanic [18] systems with moving [19] or time-dependent [20] elements. Particularly in the realm of photonics, they have been utilized to design revolutionary device applications, including but not limited to topological laser [21], topological one-way fiber [22], and topological antenna [23].

More interestingly, recent theories and experiments reported another counterintuitive circumstance as a consequence of a modified Haldane model [24,25], where the edge states at two parallel strip edges propagate in the same direction and transport forwards in a backreflection-free way, they thus are named as antichiral one-way edge states. So far, topological one-way edge states brought via these two correlated Haldane models with time-reversal symmetry breaking are still the most reliable solutions for robust unidirectional energy transmission [13,15,16,24–30], because they provide truly unidirectional, backscattering-immune energy transport at the strip edge. However, this behavior inherently limits the high-throughput robust energy transmission to a relatively low level, because only a small area around the strip edge is utilized to collect and transfer energy, which also greatly sacrifices the space utilization of sample. Undoubtedly, the implementation of one-way transmission in a large area rather than only limited at an edge is of great significance not only to open new arenas of topological physics, but also to renovate the design philosophy of robust energy transmission applications.

In this Letter, we propose a two-dimensional heterogeneous Haldane model to implement robust one-way bulk states where the energy is confined and unidirectionally transmitted in the strip bulk instead of the strip edge. We perform an *ab initio* theoretical calculation for the band structure of a zigzag ribbon via the celebrated Haldane, modified Haldane, and heterogeneous Haldane Hamiltonians to observe the evolution of topological states. We find that the heterogeneous Haldane model not only inherits the topological property from the Haldane model, but also induces the unique robust one-way bulk states. By analogy with the heterogeneous Haldane model, we further carry out the numerical simulation and experimental measurement to verify the appearance of robust one-way bulk states and their transport robustness against metallic obstacles in the strip bulk by establishing a two-dimensional microwave gyromagnetic photonic crystal. Finally, as a prototypical example, we apply our findings to exhibit a robust one-way transmission line of long-distance, large-area, and high-throughput.

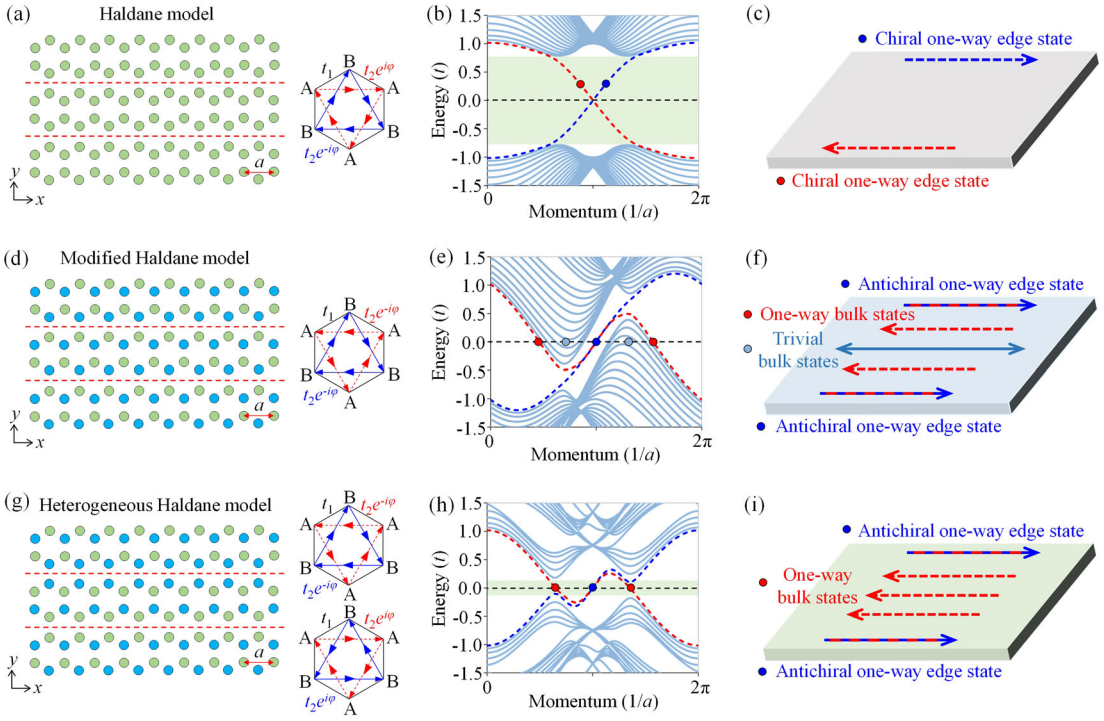

FIG. 1. Schematic of three correlated Haldane models and corresponding topological states. (a)–(c) Haldane model. (d)–(f) Modified Haldane model. (g)–(i) Heterogeneous Haldane model. (a),(d),(g) Lattice schematics. The lattice constant a is the distance between AA or BB pairs. (b),(e),(h) Band structures of zigzag strip are calculated by Haldane Hamiltonians. t_1 is taken as the unit of energy, $t_2 = 0.15$. There are no trivial bidirectional bulk states in the green regions. (c),(f),(i) Schematic diagrams of topological states.

Haldane model.—The celebrated Haldane model on a honeycomb lattice is a paradigmatic example of a Hamiltonian exhibiting the existence of electronic one-way edge states in the bandgap by connecting the quantum Hall effect and the band structure topology. The Haldane model, with time-reversal symmetry breaking next-nearest-neighbor hopping, is defined by the Hamiltonian [4,30]

$$H = t_1 \sum_{\langle i,j \rangle} c_i^\dagger c_j + t_2 \sum_{\langle\langle i,j \rangle\rangle} e^{-i v_{ij} \varphi} c_i^\dagger c_j + \text{H.c.}, \qquad (1)$$

where t_1 and t_2 are the nearest-neighbor hoppings and next-nearest-neighbor hoppings respectively. The latter containing additional phases $v_{ij}\varphi$ are defined along the arrows shown in Fig. 1(a), here $\varphi = \pi/2$, and $v_{ij} = \pm 1$ corresponds to the clockwise or counterclockwise hopping of the A or B site in the honeycomb lattice. $c_i^\dagger$ and c_i are the creation and annihilation operators at site i, i and j run over all sites in the system. When the next-nearest-neighbor hoppings of two sublattices A and B are unequal [$v_{ij} = \pm 1$, see Fig. 1(a)], the degeneracy of Dirac points is lifted up, leading to a full band gap (green region). As shown in Fig. 1(b), there exist two one-way edge states (red and blue dots) that connect two Dirac points, and one edge state propagates rightwards (blue dot) and the other propagates leftwards (red dot) [see Fig. 1(c)], as expected of the well-studied chiral one-way edge states.

Modified Haldane model.—On the contrary, recent theories reported a modified Haldane model [24] that makes the next-nearest-neighbor hoppings of two sublattices A and B equal [i.e. $v_{ij} = +1$ or $v_{ij} = -1$, see Fig. 1(d)]. Such a configuration maintains the degeneracy of Dirac points but induces energy shifts, leading to the identical dispersion of two edge states (blue dot), as illustrated in Fig. 1(e). These two edge states propagate in the same direction at two parallel edges and thus are called antichiral one-way edge states. As required by energy power conservation that the number of leftward and rightward states of whole system must be the same [24], there also emerge two counterpropagating associated bulk states that belong to the strip bulk and are spatially separated from the edge states. As shown in Fig. 1(e), these two associated bulk states (red dots) possess the same group velocity, so they also transport only in one direction [see Fig. 1(f)]. However, for the black dotted line at zero energy, in addition to the antichiral one-way edge states and associated one-way bulk states, it also intersects the trivial bidirectional bulk states on the valleys (baby blue dots). Thus, electrons can unidirectionally transport along the strip edges (blue dots), but they will suffer the backscattering when they move into the strip bulk due to the presence of trivial bidirectional bulk states (baby blue dot), as seen in Fig. 1(f).

Heterogeneous Haldane model.—A heterogeneous Haldane model we propose here is composed of alternately stacking two modified Haldane lattices with opposite

next-nearest-neighbor hoppings, as seen in Fig. 1(g). Figure 1(h) indicates that the heterogeneous model inherits the antichiral one-way edge states (blue dot) and associated one-way bulk states (red dots) from the modified Haldane model but separates them from the trivial bidirectional bulk states (baby blue dots). As a result, a green region that supports only two antichiral one-way edge states and two associated one-way bulk states appears near the zero energy. This result reveals that the one-way transport of electrons can occur not only along a narrow strip edge (blue dots) but also within a wide strip bulk (red dots), as illustrated in Fig. 1(i). Notably, the band structures of zigzag strip calculated by three correlated Haldane Hamiltonians of various t_2 can be seen in the Supplemental Material [31].

Gyromagnetic photonic crystal demonstration.—We use a two-dimensional air-loaded gyromagnetic photonic crystal of a honeycomb lattice operating at microwave frequencies to observe the one-way bulk states predicted by the heterogeneous Haldane model, as illustrated in Fig. 2(a) (see Supplemental Material [31] for the material and sample fabrication). There are two main reasons for this operation: (i) the theory of photonic crystals relies on an analogy between Maxwell's equations in a periodic medium and quantum mechanics with a periodic Hamiltonian, from which photonic band structures arise in a manner analogous to electronic band structures in a solid [30]. (ii) The most critical unequal next-nearest-neighbor hoppings of two sublattices A and B in the heterogeneous Haldane model can be produced by oppositely magnetizing the gyromagnetic cylinders with pairs of magnets [25].

Figure 2(b) exhibits the calculated projected band structure of heterogeneous gyromagnetic photonic crystal along the zigzag edge (x direction), by adopting a supercell consisting of thirteen honeycomb lattices in one column, and the lattice constant is $a = 20.0$ mm. Four dispersion curves appear inside the yellow region ranging from 5.25 to 5.40 GHz, and among them, two dispersion curves are degenerated and possess the identical dispersion behavior around $k_x = 0.5$ $(2\pi/a)$. The eigenmodal field profiles illustrated in Fig. 2(e) show that there are two bulk states (states 1 and 4) whose electric fields are dispersed uniformly in the strip bulk and two edge states (states 2 and 3) whose electric fields are concentrated on the strip edge (see Supplemental Material [31] for the transition between edge state and bulk state at the extreme of the dispersion curves). As the slope signs of edge states are positive while that of bulk states are negative, the edge states and bulk states will unidirectionally propagate rightwards and leftwards, respectively. Notably, the electric field distributions of one-way edge states and one-way bulk states are almost spatially separated, making it possible that the one-way edge states and one-way bulk states can be selectively excited under the suitable excitation conditions. Besides, these one-way states are below the light cone, meaning that they will not be coupled into the air background and result

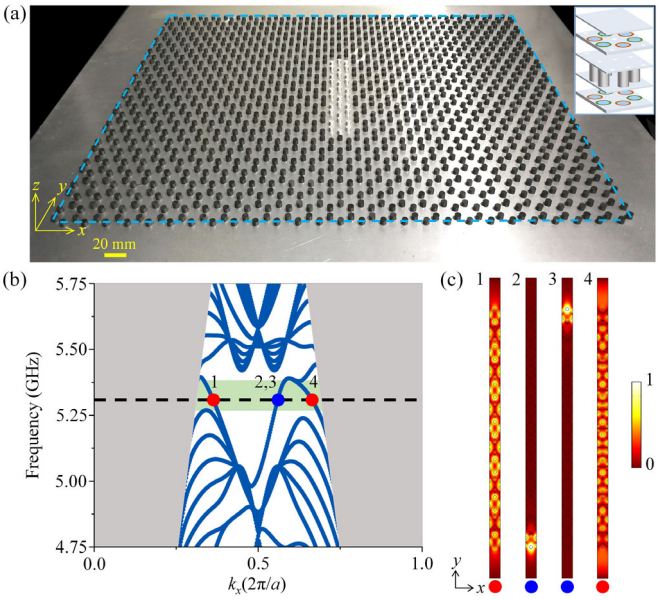

FIG. 2. Experimental sample, projected band structure and eigenmodal field of heterogeneous gyromagnetic photonic crystal strip. (a) Top view of the sample with the top metallic plate and magnet array is removed. The outline of whole strip is marked with a blue dashed line. The gyromagnetic cylinders in the middle of strip bulk are replaced with metallic cylinders of the same size that are used to verify the transport robustness of one-way bulk states. The inset is the illustration of the experimental system. (b) Projected band structure. The frequency range of the green region is $5.25 \sim 5.40$ GHz and the gray regions are light cone. (c) Eigenmodal field profiles of states 1–4.

in leakage when propagating forwards, so that this heterogeneous gyromagnetic photonic crystal does not need the ancillary cladding layer made of either a perfect metal or band gap photonic crystal to confine the energy to propagate in the strip edge and strip bulk.

Robust one-way bulk states.—The experimental results of electric-field mapping displayed in Fig. 3(a) illustrate that when a plane wave at 5.30 GHz is incident from the left port, its energy transmission is forbidden. However, when the plane wave is incident from the right port, its energy can pass through the strip bulk, showing the one-way bulk state transport, as illustrated in Fig. 3(b). This one-way property also can be demonstrated in the measured transmission spectra of Fig. 3(d) where there exists a strong nonreciprocity between 5.25 and 5.40 GHz, with a 30–35 dB difference between the rightward and leftward transmissions. Next, we proceed to verify the transport robustness of these one-way bulk states in the presence of metallic obstacles on the transport path. The metallic obstacles are formed by replacing five honeycomb lattices of gyromagnetic cylinders with the metallic cylinders of same size in the strip bulk, as shown in Fig. 2(a). The measured electric field intensity distributions show that right-incident energy can bypass the metallic obstacles and propagate forwards almost without backscattering, as seen

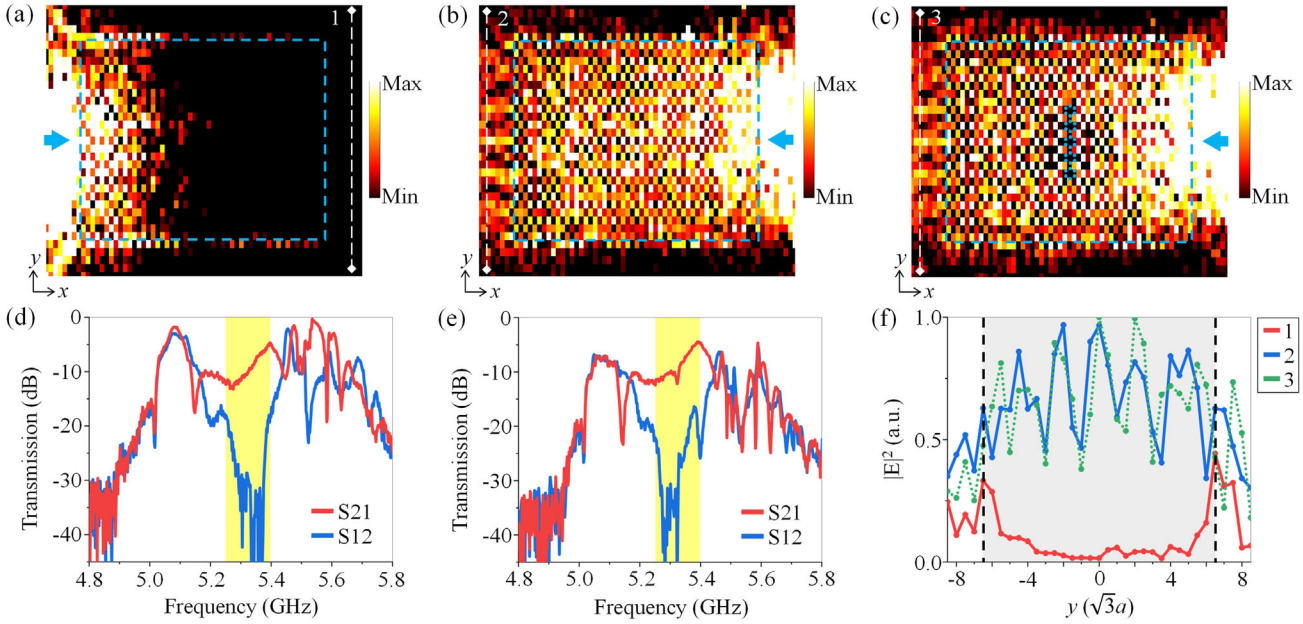

FIG. 3. Measured electric field intensity distributions and transmission spectra of robust one-way bulk states. Electric field distributions excited by (a) left-incident plane wave, (b) right-incident plane wave, and (c) right-incident plane wave when the gyromagnetic cylinders of five honeycomb lattices in the strip bulk are replaced by the metallic cylinders of the same size [blue circles, see also Fig. 2(a)]. Measured transmission spectra with (d) no metallic obstacle and (e) metallic obstacles in the strip bulk. The frequency range of yellow regions is 5.25 ~ 5.40 GHz. S21 and S12 represent the transmission coefficients of leftward and rightward propagation, respectively. (f) Measured electric intensity profiles along the white dotted lines 1–3 in (a)–(c). The gray region indicates the strip bulk and the two black dotted lines represent the strip edge.

in Fig. 3(c). Figure 3(e) illustrates that the bulk states at the frequency range of 5.25 ~ 5.40 GHz (yellow region) still remain a strong nonreciprocity, indicating that these bulk states are insensitive to the metallic obstacles in the strip bulk. Figure 3(f) exhibits the electric field intensity distributions measured by point-by-point along the white dotted lines 1, 2 and 3 in Figs. 3(a)–3(c). These measured results provide the direct and strong evidence of the robust one-way transport of bulk states, and they are in agreement with the theoretical prediction and the simulated data supported in Supplemental Material [31]. The difference between the realized heterogeneous Haldane model in photonics and the theoretically proposed heterogeneous Haldane model in electronics is also discussed in Supplemental Material [31]. To make a more direct comparison, we also calculate the projected band structure, eigenmodal field, and electromagnetic wave transport behavior of antichiral gyromagnetic photonic crystal originated from the modified Haldane model (see Supplemental Material [31]).

Beyond the one-way transport, these results also imply the possibility of implementing the robust transmission line with long distance, large area, and high throughput in a two-dimensional open space. As a prototypical example, we further investigate the transport behaviors of electromagnetic waves in a strip with a very long length of $100a$, and the simulation results are illustrated in Fig. 4. The excitation frequency of the right-incident plane wave (blue arrow) is 5.30 GHz. The simulated electric field distribution shown in Fig. 4(a) illustrates that the energy fluxes are confined on the strip bulk and travel forward in a backreflection-free way. Although there exist metallic obstacles in the strip bulk, the whole strip still can be entirely lightened by the right-incident plane wave as the electric field can recover its original distributions after climbing over the metallic obstacles, as seen in Figs. 4(b) and 4(c). Figure 4(d) shows that the electric field intensities along the white dotted lines 1–3 remain the same in the unperturbed, weak perturbed, and strong perturbed cases. We proceed to plot the electric field intensities of white dotted lines a–f illustrated in Fig. 4(e), which show that the electric field distributions along the lines a–f are almost identical, and the ideal transmission efficiencies of the one-way bulk state are more than 98.0%. These results show that although the antichiral edge states with nonzero overlap with the one-way bulk states can act as a scattering channel, they mainly prevent the external electromagnetic waves from directly coupling into the strip through the upper and lower edges of the interface between air and gyromagnetic photonic crystal. Besides, once the one-way bulk states are excited, they can maintain the excellent one-way transport property during the transmission process, because the electric field distributions of antichiral edge states and one-way bulk states are almost spatially separated.

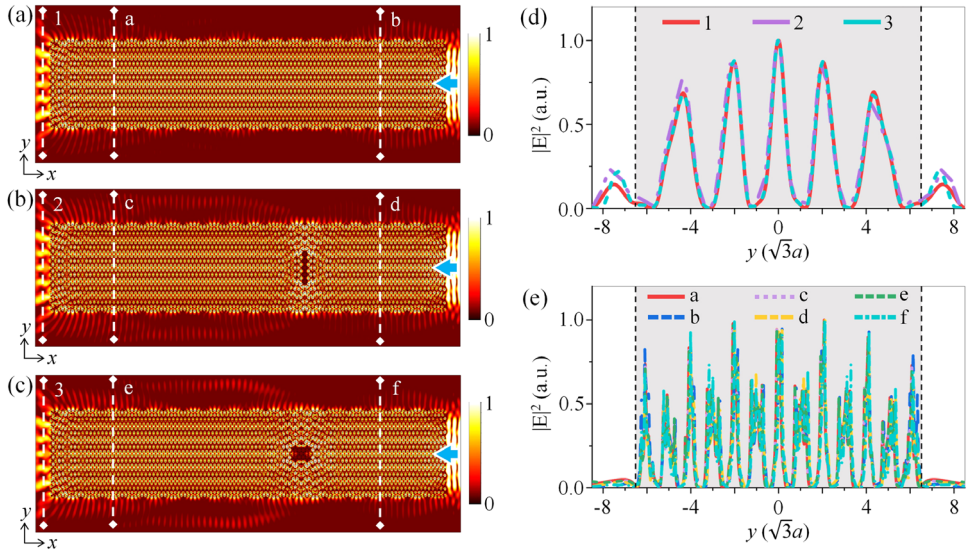

FIG. 4. Simulated electric field intensity distributions of robust one-way bulk states in a strip with a length of $100a$. (a) There are no metallic obstacles. (b) The gyromagnetic cylinders of five honeycomb lattices are replaced by metallic cylinders of the same size in the strip bulk. (c) An "X" shape array of gyromagnetic cylinders in the strip bulk is replaced by metallic cylinders of the same size. (d) Simulated electric intensity profiles along the white dotted lines 1–3 in (a)–(c). (e) Simulated electric intensity profiles along the white dotted lines a–f in (a)–(c). The gray region indicates the strip bulk and the black dotted lines represent the strip edges.

Conclusion and discussion.—We have proposed a heterogeneous Haldane model and predicted the appearance of robust one-way bulk states in a two-dimensional electronic system by using the *ab initio* theoretical calculation. By analogy with the heterogeneous Haldane model, we also have constructed a two-dimensional microwave gyromagnetic photonic crystals biased by external magnetic fields to numerically confirm and experimentally observe the existence of robust one-way bulk states in photonics. Our Letter thus provides strong support for the generalization and application of band theories to fermionic and bosonic systems with genuine topological properties, and opens a regime for developing high-throughput robust energy transmission applications in various physical settings. If this model can be implemented in some still-unknown electronic materials systems, then the resistance-free and backscattering-immune electric conductor transmission line of large current capacity might become reality by invoking the principle of powerful topology physics.

The authors are grateful for the financial support from the National Natural Science Foundation of China (11974119), Science and Technology Project of Guangdong (2020B010190001), Guangdong Innovative and Entrepreneurial Research Team Program (2016ZT06C594), and National Key R&D Program of China (2018YFA 0306200).

*Corresponding author.
phzyli@scut.edu.cn

[1] M. Z. Hasan and C. L. Kane, Colloquium: Topological insulators, Rev. Mod. Phys. **82**, 3045 (2010).
[2] X. L. Qi and S. C. Zhang, Topological insulators and superconductors, Rev. Mod. Phys. **83**, 1057 (2011).
[3] C. K. Chiu, J. C. Y. Teo, A. P. Schnyder, and S. Ryu, Classification of topological quantum matter with symmetries, Rev. Mod. Phys. **88**, 035005 (2016).
[4] F. D. M. Haldane, Model for a Quantum Hall Effect without Landau Levels: Condensed-Matter Realization of the "Parity Anomaly", Phys. Rev. Lett. **61**, 2015 (1988).
[5] C. L. Kane and E. J. Mele, Z2 Topological Order and the Quantum Spin Hall Effect, Phys. Rev. Lett. **95**, 146802 (2005).
[6] J. Li, R. L. Chu, J. K. Jain, and S. Q. Shen, Topological Anderson Insulator, Phys. Rev. Lett. **102**, 136806 (2009).
[7] L. H. Wu and X. Hu, Scheme for Achieving a Topological Photonic Crystal by Using Dielectric Material, Phys. Rev. Lett. **114**, 223901 (2015).
[8] C. W. Peterson, W. A. Benalcazar, T. L. Hughes, and G. Bahl, A quantized microwave quadrupole insulator with topologically protected corner states, Nature (London) **555**, 346 (2018).
[9] Y. Liu, S. Leung, F. F. Li, Z. K. Lin, X. Tao, Y. Poo, and J. H. Jiang, Bulk–disclination correspondence in topological crystalline insulators, Nature (London) **589**, 381 (2021).
[10] S. Stützer, Y. Plotnik, Y. Lumer, P. Titum, N. H. Lindner, M. Segev, M. C. Rechtsman, and A. Szameit, Photonic topological Anderson insulators, Nature (London) **560**, 461 (2018).
[11] E. Lustig, S. Weimann, Y. Plotnik, Y. Lumer, M. A. Bandres, A. Szameit, and M. Segev, Photonic topological insulator in synthetic dimensions, Nature (London) **567**, 356 (2019).
[12] L. W. Clark, N. Schine, C. Baum, N. Jia, and J. Simon, Observation of Laughlin states made of light, Nature (London) **582**, 41 (2020).

[13] Z. Zhang, P. Delplace, and R. Fleury, Superior robustness of anomalous non-reciprocal topological edge states, Nature (London) **598**, 293 (2021).
[14] S. Klembt, T. H. Harder, O. A. Egorov, K. Winkler, R. Ge, M. A. Bandres, M. Emmerling, L. Worschech, T. C. H. Liew, M. Segev, and C. Schneider, Exciton-polariton topological insulator, Nature (London) **562**, 552 (2018).
[15] Z. Wang, Y. Chong, J. D. Joannopoulos, and M. Soljačić, Observation of unidirectional backscattering-immune topological electromagnetic states, Nature (London) **461**, 772 (2009).
[16] Y. Poo, R. X. Wu, Z. Lin, Y. Yang, and C. T. Chan, Experimental Realization of Self-Guiding Unidirectional Electromagnetic Edge States, Phys. Rev. Lett. **106**, 093903 (2011).
[17] H. He, C. Qiu, L. Ye, X. Cai, X. Fan, M. Ke, F. Zhang, and Z. Liu, Topological negative refraction of surface acoustic waves in a Weyl phononic crystal, Nature (London) **560**, 61 (2018).
[18] R. Süsstrunk and S. D. Huber, Observation of phononic helical edge states in a mechanical topological insulator, Science **349**, 47 (2015).
[19] A. Souslov, B. C. van Zuiden, D. Bartolo, and V. Vitelli, Topological sound in active-liquid metamaterials, Nat. Phys. **13**, 1091 (2017).
[20] R. Fleury, A. B. Khanikaev, and A. Alù, Floquet topological insulators for sound, Nat. Commun. **7**, 11744 (2016).
[21] B. Bahari, A. Ndao, F. Vallini, A. E. Amili, Y. Fainman, and B. Kanté, Nonreciprocal lasing in topological cavities of arbitrary geometries, Science **358**, 636 (2017).
[22] L. Lu, H. Gao, and Z. Wang, Topological one-way fiber of second Chern number, Nat. Commun. **9**, 5384 (2018).
[23] B. Bahari, L. Hsu, S. H. Pan, D. Preece, A. Ndao, A. E. Amili, Y. Fainman, and B. Kanté, Photonic quantum Hall effect and multiplexed light sources of large orbital angular momenta, Nat. Phys. **17**, 700 (2021).
[24] E. Colomés and M. Franz, Antichiral Edge States in a Modified Haldane Nanoribbon, Phys. Rev. Lett. **120**, 086603 (2018).
[25] P. Zhou, G. G. Liu, Y. Yang, Y. H. Hu, S. Ma, H. Xue, Q. Wang, L. Deng, and B. Zhang, Observation of Photonic Antichiral Edge States, Phys. Rev. Lett. **125**, 263603 (2020).
[26] M. C. Rechtsman, J. M. Zeuner, Y. Plotnik, Y. Lumer, D. Podolsky, F. Dreisow, S. Nolte, M. Segev, and A. Szameit, Photonic Floquet topological insulators, Nature (London) **496**, 196 (2013).
[27] G. Jotzu, M. Messer, R. Desbuquois, M. Lebrat, T. Uehlinger, D. Greif, and T. Esslinger, Experimental realization of the topological Haldane model with ultracold fermions, Nature (London) **515**, 237 (2014).
[28] Y. Ding, Y. Peng, Y. Zhu, X. Fan, J. Yang, B. Liang, X. Zhu, X. Wan, and J. Cheng, Experimental Realization of Acoustic Chern Insulators, Phys. Rev. Lett. **122**, 014302 (2019).
[29] T. Hofmann, T. Helbig, C. H. Lee, M. Greiter, and R. Thomale, Chiral Voltage Propagation and Calibration in a Topolectrical Chern Circuit, Phys. Rev. Lett. **122**, 247702 (2019).
[30] F. D. M. Haldane and S. Raghu, Possible Realization of Directional Optical Waveguides in Photonic Crystals with Broken Time-Reversal Symmetry, Phys. Rev. Lett. **100**, 013904 (2008).
[31] See Supplemental Material at http://link.aps.org/supplemental/10.1103/PhysRevLett.128.257401 for the band structures calculated by three Haldane Hamiltonians of various t_2, the material characteristics, the experimental sample and setup, the numerical simulation and experimental measurement, the transition between edge state and bulk state, the simulated electric field intensity distributions of one-way bulk states, the simulated results of antichiral gyromagnetic photonic crystal, and the difference between heterogeneous Haldane model in electronics and photonics.